Carbohydrate Polymers 87 (2012) 2464–2469

Contents lists available at SciVerse ScienceDirect

Carbohydrate Polymers

journal homepage: www.elsevier.com/locate/carbpol

Bacterial cellulose reinforced polyurethane-based resin nanocomposite: A study of how ethanol and processing pressure affect physical, mechanical and dielectric properties

J. Juntaro [a], S. Ummartyotin [b], M. Sain [a,**], H. Manuspiya [b,*]

[a] Centre for Biocomposites and Biomaterials Processing, Faculty of Forestry, University of Toronto, 33 Willcocks Street, Toronto M5S 3B3, Canada
[b] The Petroleum and Petrochemical College, Center of Excellence for Petroleum, Petrochemicals and Advanced Materials Chulalongkorn University, Bangkok 10330, Thailand

ARTICLE INFO

Article history:
Received 21 June 2011
Received in revised form 21 October 2011
Accepted 7 November 2011
Available online 15 November 2011

Keywords:
Bacterial cellulose
Nanocomposite
Physical
Mechanical
Dielectric

ABSTRACT

Nanocomposite films of bacterial cellulose (10–50 wt%) and polyurethane-based resin were prepared and characterized for physical, mechanical and dielectric properties. It was observed that the bacterial cellulose swelled in ethanol, and that bacterial cellulose sheets prepared from fibre suspension in ethanol exhibited a relatively less dense structure in comparison to those processed from aqueous fibre suspension. Nanocomposites fabricated from ethanol suspension also showed inferior mechanical properties but superior dielectric properties. Higher amounts of free proton generated from ethanol can induce more dipole mechanism; therefore, there is higher mobility of proton localized along cellulose chain, indicating that higher dielectric constants can be obtained.

1. Introduction

Nano-scale cellulose has emerged as a green reinforcement for the design of nanocomposites due to its outstanding mechanical properties (Gindl & Keckes, 2005; Grunert & Winter, 2002; Klemm et al., 2006; Kramer et al., 2006; Mohanty, Misra, & Drzal, 2005; Nakagaito, Iwamoto, & Yano, 2005a; Valadez-Gonzalez, Cervantes-Uc, Olayo, & Herrera-Franco, 1999; Yano et al., 2005). Nanocellulose can be extracted from wood, tunicate (Favier, Chanzy, & Cavaille, 1995) and products of some bacteria strains (Basta & El-Saied, 2009). Among these cellulose sources, the production of nanocellulose from products of bacteria requires less energy consumption, along with fewer chemical and physical treatment steps. Currently, bacterial cellulose is used in food, specialty paper, speaker membranes and biomedical applications such as wound dressings and artificial skin (Iguchi, Yamadaka, & Budhiono, 2000). Bacterial cellulose has remarkable properties. It has ribbon shape with diameters ranging from 8 to 50 nm which is about a thousand times smaller than that of common plant fibre's (10–600 μm) (Basta & El-Saied, 2009). The fibril is composed of a bundle of much finer microfibrils of 2–4 nm in diameter (Nakagaito & Yano, 2005). It has a high degree of crystallinity, degree of polymerization, purity and specific area (Yoshinaga, Tonouchi, & Watanabe, 1997). Renewable bacterial cellulose-reinforced nanocomposites already show promising mechanical properties (Gindl & Keckes, 2005; Grunert & Winter, 2002; Nakagaito et al., 2005a; Orts et al., 2005).

Recent studies disclosed the potential of nanocellulose as substrates for flexible optoelectronic and photonic devices (Legnini et al., 2008; Nogi & Yano, 2008; Okahisa, Yoshida, Miyagushi, & Yano, 2009). Legnini et al. (2008) demonstrated organic light emitting diode (OLED) devices based on flexible bacterial cellulose membrane. The maximum luminance was measured to be 1200 cd/m^2. Okahisa et al. (2009) also reported the successful fabrication of OLED displays on a flexible nanocomposite of cellulose and acrylic resin. Similar works also include Yano et al. (2005), Nogi and Yano (2008) and Nakagaito, Iwamoto, and Yano (2005b). Nanocellulose plays a vital role in improving mechanical properties and dimensional stability of the substrates. The Young's modulus of bacterial cellulose fibril is as high as 114 GPa (Hsieh, Yano, Nogi, & Eichhorn, 2008), which is almost twice of Young's modulus of aramid fibre (63–67 GPa (Bledzki, Reihmane, & Gassan, 1996; Saechtling, 1987)). The coefficient of thermal expansion of nanocellulose fibril in the axial direction is very low, at only 0.1 ppm/K (Nishino, Matsuda, & Hirao, 2004).

In this work, we wish to report a nanocomposite prepared from ethanol-treated nanocellulose composite, impregnated with polyurethane (PU) based resin; its potential as a flexible substrate for electronic devices was investigated. The PU based resin was

* Corresponding author. Tel.: +66 2 2184101; fax: +66 2 215 4459.
** Corresponding author. +1 416 9463191; fax: +1 416 978 3834.
E-mail addresses: m.sain@utoronto.ca (M. Sain), hathaikarn.m@chula.ac.th (H. Manuspiya).

0144-8617/$ – see front matter © 2011 Elsevier Ltd. All rights reserved.
doi:10.1016/j.carbpol.2011.11.020

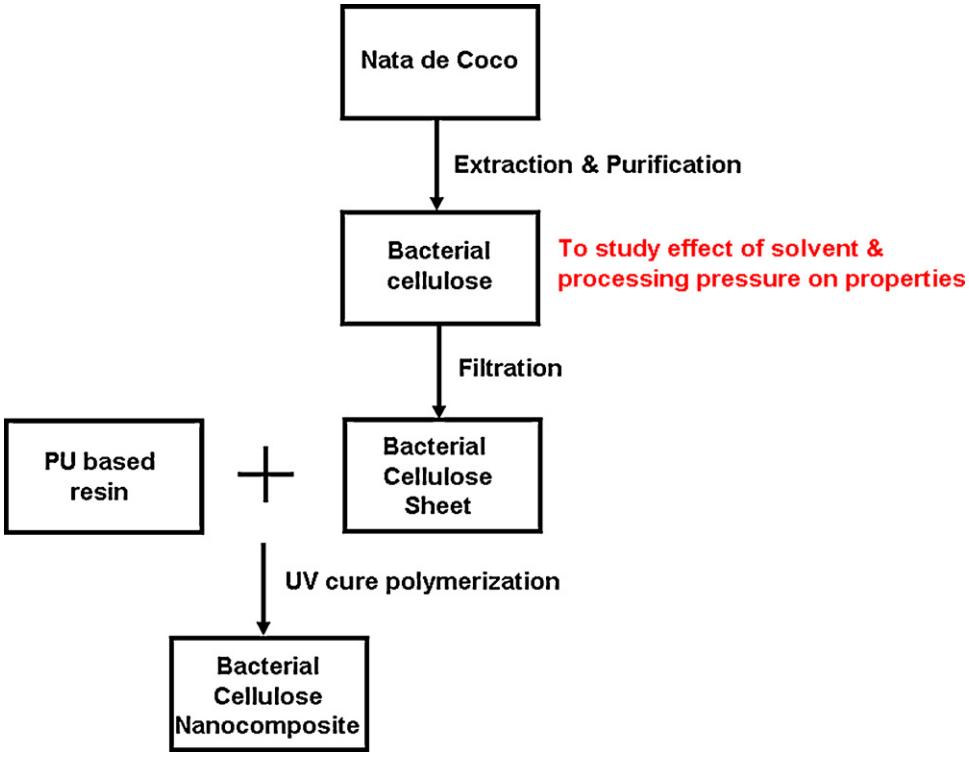

Fig. 1. The diagram of bacterial cellulose nanocomposite preparation.

chosen due to its unique set of potentials, including its transparency, flexibility, ability to withstand the weather, scratching, abrasion and chemical resistances (Chattopadhyay & Raju, 2007). The incorporation of bacterial cellulose into PU based resin will enhance the performance of the nanocomposites in terms of physical, mechanical and dielectric properties.

2. Materials and methods

2.1. Materials

PU based resins were purchased from Sartomer Company, Inc. (Exton, PA, USA). The resin has the density of 1.16 g/cm^3. It was stored in dark room due to its light sensitivity. Irgacure 184 and Irgacure 819 were used as UV curing catalyst. Bacterial cellulose was extracted from the commercially available Nata de coco (Uno Foods, BC, Canada), an indigenous Filipino-originated dessert of which the main components were regarded as bacterial cellulose (Basta & El-Saied, 2009; Iguchi et al., 2000; Jagannath, Kalaiselvan, Manjunatha, Raju, & Bawa, 2008). Characterizations of bacterial cellulose extracted from Nata de coco were reported (Juntaro, 2009); its characteristics matched those of bacterial cellulose extracted from the culture of *Acetobacter xylinum*. Analytical grade ethanol was purchased from Bioshop Canada Inc. at the University of Toronto. All chemicals were used as received.

2.2. Methods

2.2.1. Extraction and purification of bacterial cellulose

Bacterial cellulose was extracted from Nata de coco. The coconut gel content was first washed with distilled water and cut into small pieces using a laboratory blender. In order to purify the bacterial cellulose, the bacterial cellulose suspension was treated with 0.1 M NaOH solution at 80 °C for 20 min to remove any remaining microorganisms, medium component and soluble polysaccharides following Toyosaki et al. (1995). The cellulose was then separated from the NaOH solution by filtering through a Buchner funnel fitted with fritted disc (10–15 μm porosity), which was connected to a Buchner flask and a vacuum pump. The cellulose was thoroughly washed with distilled water until neutral pH.

2.2.2. Fabrication of nanocomposite sheets

To fabricate the nanocomposite sheet, nanocellulose sheet was first fabricated through three different methods;

Sample A – From 250 ml of bacterial cellulose suspension in water, the water was removed through filtration with a Buchner funnel fitted with a polyterafluoroethylene membrane filter (0.1 μm mesh, 90 mm diameter), which was connected to a Buchner flask and a vacuum pump. The concentration of the bacterial cellulose in the water suspension was adjusted to achieve a dried bacterial cellulose disc of 0.25 g. The filtration was carried on until the water was removed from the bacterial cellulose as much as possible, which subsequently resulted in a wet sheet of bacterial cellulose. Such a wet sheet was then dried between two polyterafluoroethylene membranes under the applied pressure of 58 psi (400 KPa), following the paper handsheet formation standard SCAN C 26:76.

Sample B – Same as Sample A, but the wet sheet of bacterial cellulose was dried under the applied pressure of 1 psi. The applied pressure of 1 psi was chosen here to achieve the bacterial cellulose sheet with less dense fibre structure and higher free volume.

Sample C – Same as Sample B, but the bacterial cellulose suspension in water was solvent-exchanged into ethanol prior to the Buchner filtration.

After Sample A, Sample B and Sample C were completely dried, they were impregnated with the PU resin for 1 min and cured under UV (300 nm) at 25 mW/cm^2 for 3 min. As a reference, the neat PU resin sheet was also fabricated in similar manner. The thickness of all samples was in the range of 0.3–0.5 mm. From hereon, the nanocomposites fabricated from Samples A, B, and C will be referred to as Nanocomposites A, B, and C accordingly. 0.1 wt% of Irgacure

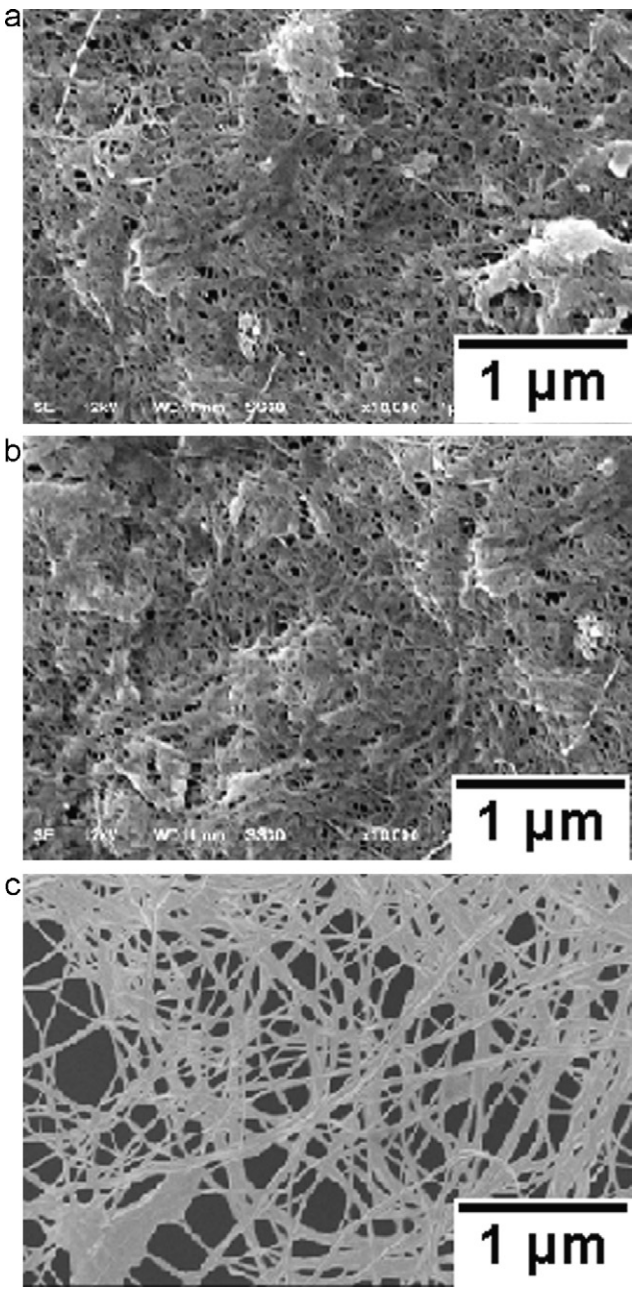

Fig. 2. SEM micrographs of bacterial cellulose sheet (A) Sample A: drying from aqueous suspension under 58 psi, (B) Sample B: drying from aqueous suspension under 1 psi and (C) Sample C: drying from ethanol suspension under 1 psi.

184 and 0.01 wt% of Irgacure 819 were used as UV curing catalyst. All experiments involving the PU based resin were conducted in a dark room as the resin was sensitive to light.

The diagram of bacterial cellulose nanocomposite preparation was exhibited as in Fig. 1.

2.2.3. Determination of morphological properties

Morphological properties can be determined by scanning electron microscope (JOEL JSM-6301F). It operated at an acceleration voltage of 15 kV. The samples were stored in desiccators for humidity prevention. Then, each sample was place on the carbon tape and sputtered with gold particles prior to analysis.

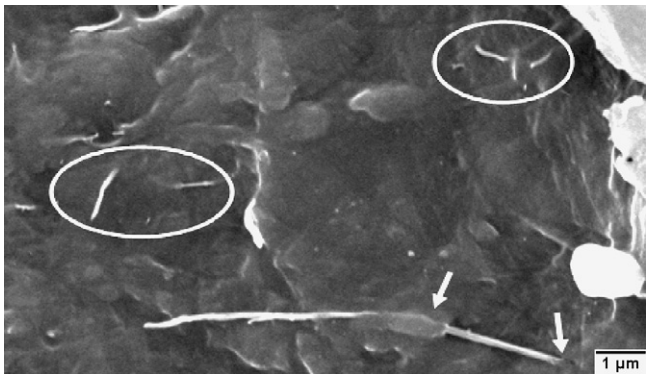

Fig. 3. SEM of bacterial cellulose sheet partially impregnated with the PU-based resin.

2.2.4. Determination of tensile properties

The tensile tests were conducted in accordance to the ISO Standard number ISO 527:1996. The sample was cut with a Zwick cutter into dog-bone specimen type 5A. The samples had the overall length and the gauge length of 75 and 20 mm, respectively. The initial distance between grips was 50 mm and its width at the grip end was 12.5 mm. The width at the narrowest part was 4 mm and the thickness was 0.3–0.5 mm. The testing speed was 1 mm/min. The specimens were preconditioned at 20 °C in 54% relative humidity in a desiccator containing a saturated solution of $Mg(NO_3)_2$ for at least 48 h prior to testing. The tensile test were conducted using as Instron universal material testing machine (Instron 4502, Instron Corporation, MA, USA) equipped with a 1 kN load cell. At lease 5 specimens were tested per sample to obtain a statistical average.

2.2.5. Determination of dielectric properties

Dielectric constant and dielectric loss were measured by a precision LCR meter (Agilent E4980A) at ambient temperature and various frequencies (1–100 kHz). The samples were coated by silver paint as electrode on both sides before measurement.

3. Results and discussion

3.1. Morphological properties

Bacterial cellulose sheet produced with different methods clearly showed different fibre structures. SEM of bacterial cellulose sheet shows cellulose nanofilaments ranging from 50 to 100 nm in diameter (Fig. 2). The orientation of bacterial cellulose exhib-

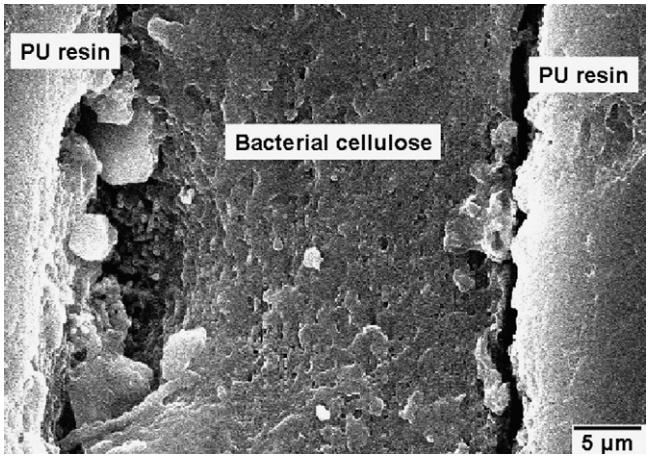

Fig. 4. Cross sectional SEM image of bacterial cellulose prepared from Sample A and PU-based rein.

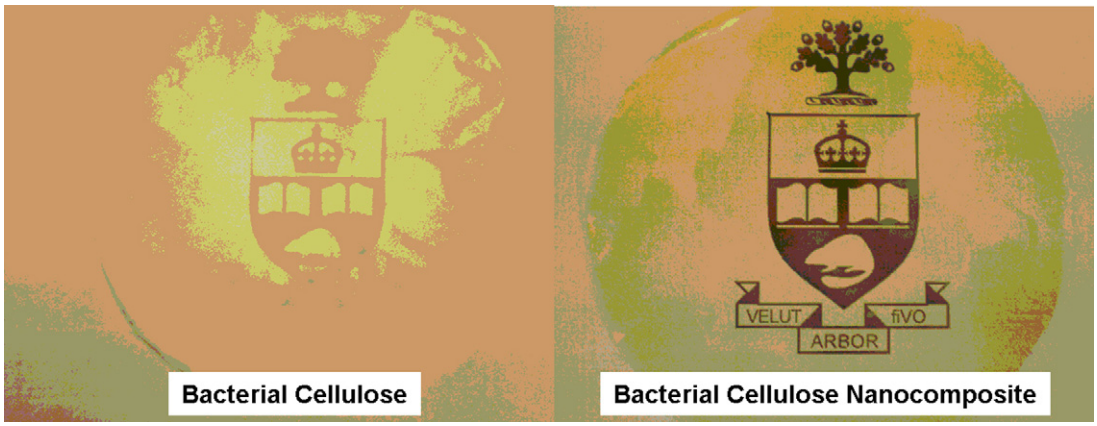

Fig. 5. Optical transparencies of Sample A and its nanocomposite.

ited three dimensional network structures. The sheet from Sample A (58 psi, water-based suspension) showed denser fibre network structure than the sheet from Sample B (1 psi, water-based suspension), which can be ascribed to the high pressure applied during drying. The fibre network structure of the sheet from Sample C (1 psi, ethanol-based suspension) was the least dense, implying that water and ethanol environments have different effects upon the behavior of bacterial cellulose fibrils. Ethanol has higher polarity than water. It can attach to the hydroxyl groups of cellulose chains, and result in repulsive force acting among cellulose fibrils, disrupting the cohesion among cellulose chains. It could be clearly observed during the wet sheet formation that bacterial cellulose swelled in ethanol, and thus yielded the dried sheet with less fibre structure density.

The fibre structure density of the dried bacterial cellulose sheet also determined the fibre contents of the fabricated nanocomposites. Bacterial cellulose sheet can be considered as a three-dimensional network of fibres, with air interstices in between. As the bacterial cellulose sheet was impregnated with resin, these air interstices were filled by the resin. Therefore, cellulose sheet with higher fibre structure density will have lower amount of resin filled, leading to nanocomposite with higher fibre content. Nanocomposite A had fibre content of 51 wt%, while Nanocomposite B and Nanocomposite C had fibre contents of 36 wt% and 31 wt% respectively.

To investigate the compatibility between the PU-based resin and bacterial cellulose, the bacterial cellulose sheet was partially impregnated with the PU-based resin and cured. The SEM revealed good wetting between the cellulose fibre and the PU-based resin (Fig. 3). It can be observed that there was no gap between the fibre and the resin.

Consequently, Fig. 4 exhibits the cross sectional SEM image of bacterial cellulose sheet and PU-based resin. The structure of nanocomposite is the sandwich-like, composed of bacterial cellulose sheet encapsulated by PU-based resin on both sides. It is important to note that PU-based resin can be acted both as water prevention and mechanical properties enhancement to bacterial cellulose sheet.

Fig. 5 shows photographs of bacterial cellulose sheet and Nanocomposite A. The transparency of the bacterial cellulose nanocomposite confirmed good compatibility between bacterial cellulose and the resin. Theoretically, when light travels through two elements of different refractive index (RI), light diffracts. Bacterial cellulose sheet was opaque because light diffracted at the interface between cellulose and air interstices. Note that the RI of air is 1.000, the RI of PU-based resin in this work was in the range of 1.435–1.478 (Ummartyotin, Juntaro, Sain, & Manuspiya, 2012), while the RI of cellulose has been reported as 1.618 along the fibre axis and 1.544 in the transverse direction (Nogi & Yano, 2008); therefore, the close RI of the cellulose and the resin will lead to transparent nanocomposite. In addition, the preliminary result of percent of light transmittance by UV–vis spectroscopy of this nanocomposite was reported roughly 75–86%. The result suggested that the our nanocomposite can be qualified as transparent composite for flexible displays, cited by Choi, Kim, and Ha (2008).

If the cellulose and the PU-based resin were not compatible, there would be formation of small air gaps at the interface, leading to light diffraction and deteriorating the transparency.

3.2. Mechanical properties

Tensile properties of PU-based resin were greatly improved with the incorporation of bacterial cellulose (Figs. 6 and 7). Nanocomposite A had the highest Young's Modulus and tensile strength, followed by Nanocomposites B and C respectively. This trend was in accordance with the bacterial cellulose contents of the nanocomposites; Nanocomposite A had higher bacterial cellulose content than Nanocomposites B and C respectively. Interestingly, Young's moduli of all bacterial cellulose nanocomposites and the tensile strengths of bacterial cellulose nanocomposites type A and B exceeded those of pure bacterial cellulose sheet. As bacterial cellulose sheet was a three-dimensional network structure of fibres with

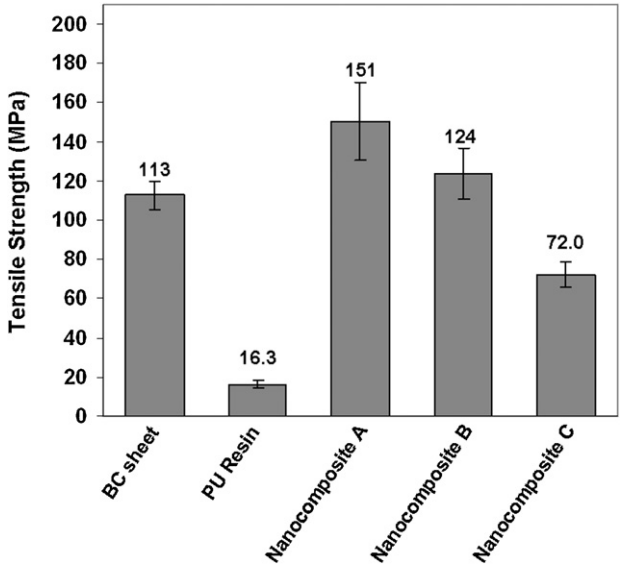

Fig. 6. Tensile strength of Samples A, B, C and their nanocomposites.

Table 1
Significant value of fibre content, tensile strength and Young's modulus of Nanocomposites A, B and C.

Nanocomposite	A	B	C
Fibre content (%)	51	36	31
Tensile strength (MPa)	151	124	72
Young modulus (GPa)	11.6	9.5	5.4

air interstices in between, when the tensile stress was applied to the bacterial cellulose sheet, the stress would be transferred through the fibre network, i.e. the stress could only be transferred 'around' the interstices, not 'through' the interstices. While in the case of the nanocomposites, these air interstices were filled with the resin matrix, enabling the stress to be transferred from fibres to fibres through the resin molecules and thus rendering better mechanical properties.

The significant value of the amount of fibre content, tensile strength and Young's modulus of Nanocomposites A, B and C was also shown in Table 1

The stress–strain curves of the neat bacterial cellulose sheet, neat PU based resin and the nanocomposites were illustrated in Fig. 8. It shows the graphical representation of the relationship between applied stress and strain derived from the sample

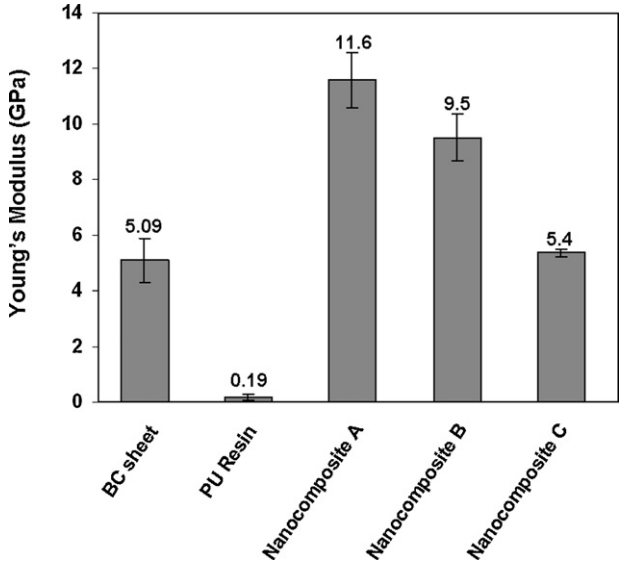

Fig. 7. Young's modulus of Samples A, B, C and their nanocomposites.

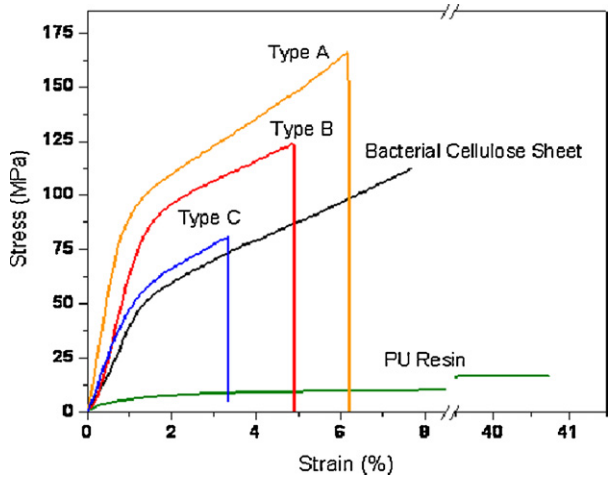

Fig. 8. Stress–strain curve of Samples A, B, C and their nanocomposites.

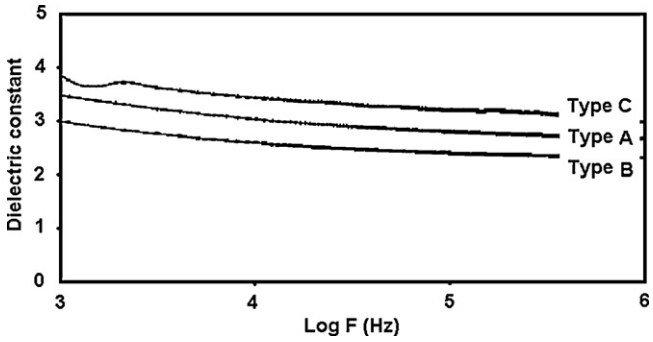

Fig. 9. Dielectric constant of Nanocomposites A, B and C.

deformation. The yield strengths of these nanocomposites were greatly enhanced with the incorporation of bacterial cellulose sheet. The ductile PU based resin became more brittle by reinforcement of bacterial cellulose sheet. Nanocomposite C exhibited lower yield strength than Nanocomposites A and B, which is in consistence with tensile strength and Young's modulus in Figs. 6 and 7.

3.3. Dielectric properties

Figs. 9 and 10 show the variation of the dielectric properties of bacterial cellulose nanocomposites. The frequency dependence of dielectric constant and dielectric loss at ambient temperature was observed. In all cases, a strong frequency dispersion of permittivity was observed in the low frequency region, followed by a nearly frequency independent characteristic with increment of frequency. The decrease of dielectric properties with increasing frequency was due to the attribution of relaxation behavior. Fig. 9 clearly represents the frequency dependence of dielectric constant. Nanocomposite C had higher dielectric constant than Nanocomposite A, followed by Nanocomposite B. As ethanol was used during the processing of bacterial cellulose sheet for Nanocomposite C, relatively higher amount of free proton was generated and trapped along nano-cellulose in comparison to Nanocomposites A and B, of which water was used for sheet formation. The higher amount of free proton suggested more localization of charge carriers along with mobile ions, resulting in higher dipole polarization and thus higher dielectric constant. The dielectric constant of Nanocomposite A was higher than that of Nanocomposite B as the bacterial cellulose sheet fabricated for Nanocomposite A was dried under higher pressure. The denser cellulose network structure of Nanocomposite A implied lower free space in the sample, leading to higher level of ion interaction and higher dielectric constant.

The frequency dependence of dielectric loss at ambient temperature is shown in Fig. 10. The relatively high dielectric loss values of Nanocomposite C suggested the presence of high amount of

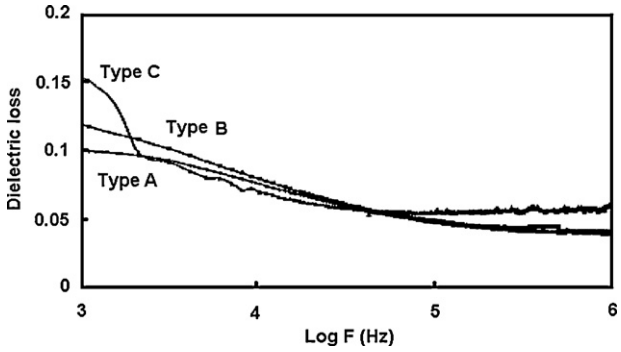

Fig. 10. Dielectric loss of Nanocomposites A, B and C.

free protons or space area among bacterial cellulose network. The dielectric loss resulted from the repulsion among proton electric charge along nanocellulose. It can be observed that the dielectric loss of Nanocomposite C was higher than those of samples fabricated from aqueous solution (i.e. Nanocomposites A and B). Nanocomposite A had lower dielectric loss that Nanocomposite B. Higher pressure in processing cellulose sheet for Nanocomposite A led to higher cellulose network density, suggesting less free space and the consequent low dielectric loss, which is consistent with the previous discussion. Mechanical properties can also be related to the presence of free space, i.e. more free space will lead to decrease in mechanical properties.

4. Conclusion

Nanocomposites of bacterial cellulose and PU based resin were successfully prepared. Bacterial cellulose showed good compatibility with PU based resin. The nanocomposite processed from aqueous fibre suspension exhibited superior density and mechanical properties to the nanocomposite processed from ethanol fibre suspension, but with inferior dielectric properties. It can be indicated that bacterial cellulose nanocomposite can be the excellent candidate for electronic display device in the near future.

Acknowledgements

The authors would like to acknowledge ABIP, NSERC Manufacturing Network and CG Tower for their financial support. Special thanks are due to Mr. Natthaphon Bunnak for dielectric properties measurement. SU would like to acknowledge the scholarship from Center of Excellence for Petroleum, Petrochemicals and Advanced Materials, Chulalongkorn University, Thailand.

References

Basta, A. H., & El-Saied, H. (2009). Performance of improved bacterial cellulose application in the production of functional paper. *Journal of Applied Microbiology*, *107*, 2098–2107.

Bledzki, A. K., Reihmane, S., & Gassan, J. (1996). Properties and modification methods for vegetable fibers for natural fiber composites. *Journal of Applied Polymer Science*, *59*, 1329–1336.

Chattopadhyay, D. K., & Raju., K. V. S. N. (2007). Structural engineering of polyurethane coatings for high performance applications. *Progress in Polymer Science*, *32*, 352–418.

Choi, M. C., Kim, Y., & Ha., C. S. (2008). Polymers for flexible displays: From material selection to device application. *Progress in Polymer Science*, *33*, 581–630.

Favier, V., Chanzy, H., & Cavaille, J. Y. (1995). Polymer nanocomposites reinforced by cellulose whisker. *Macromolecules*, *28*, 6365–6367.

Gindl, W., & Keckes, J. (2005). All-cellulose nanocomposite. *Polymer*, *46*, 10221–10225.

Grunert, M., & Winter, W. T. (2002). Nanocomposites of cellulose acetate butyrate reinforced with cellulose nanocrystals. *Journal of Polymers and The Environment*, *10*, 27–30.

Hsieh, Y. C., Yano, H., Nogi, M., & Eichhorn, S. J. (2008). An estimation of the Young's modulus of bacterial cellulose filaments. *Cellulose*, *15*, 507–513.

Iguchi, M., Yamadaka, S., & Budhiono, A. (2000). Bacterial cellulose- a masterpiece of nature's arts. *Journal of Materials Science*, *35*, 261.

Jagannath, A., Kalaiselvan, A., Manjunatha, S. S., Raju, P. S., & Bawa, A. S. (2008). The effect of pH, sucrose and ammonium sulphate concentrations on the production of bacterial cellulose (Nata-de-coco) by *Acetobacter xylinum*. *World Journal of Microbiology & Biotechnology*, *24*, 2593–2599.

Juntaro, J. (2009). *Environmentally friendly hierarchical composites*. London: Department of Chemical Engineering and Chemical Technology, Imperial College London.

Klemm, D., Schumann, D., Kramer, F., Hessler, N., Hornung, M., Schmauder, H. P., et al. (2006). Nanocelluloses as innovative polymers in research and application. *Polysaccharides II*, *205*, 49–96.

Kramer, F., Klemm, D., Schumann, D., Hessler, N., Wesarg, F., Fried, W., et al. (2006). Nanocellulose polymer composites as innovative pool for (bio)material development. *Macromolecular Symposia*, *244*, 136–148.

Legnini, C., Vilani, C., Calil, V. L., Barud, H. S., Quirino, W. G., Achete, C. A., et al. (2008). Bacterial cellulose membrane as flexible substrate for organic light emitting devices. *Thin Solid Films*, *517*, 1016–1020.

Mohanty, A. K., Misra, M., & Drzal, L. T. (Eds.). (2005). *Natural fibers, biopolymers and biocomposites*. Boca Raton, FL: CRC Press, Taylor &Francis Group.

Nakagaito, A. N., Iwamoto, S., & Yano, H. (2005a). Bacterial cellulose: the ultimate nano-scalar cellulose morphology for the production of high-strength composites. *Applied Physics A: Material Science and Processing*, *80*, 93–97.

Nakagaito, A. N., Iwamoto, S., & Yano, H. (2005b). Bacterial cellulose: the ultimate nano-scalar cellulose morphology for the production of high-strength composites. *Applied Physics A: Materials Science and Processing*, *80*, 93.

Nakagaito, A. N., & Yano, H. (2005). Novel high-strength biocomposites based on microfibrillated cellulose having nano-order-unit web-like network structure. *Applied Physics A: Materials Science and Processing*, *80*, 155–159.

Nishino, T., Matsuda, I., & Hirao, K. (2004). All-cellulose composite. *Macromolecules*, *37*, 7683–7687.

Nogi, M., & Yano., H. (2008). Transparent nanocomposites based on cellulose produced by bacteria offer potential innovation in the electronics device industry. *Advanced Materials*, *20*, 1849–1852.

Okahisa, Y., Yoshida, A., Miyagushi, S., & Yano., H. (2009). Optically transparent wood-cellulose nanocomposite as a base substrate for flexible organic light emitting displays. *Composites Science and Technology*, *69*, 1958–1961.

Orts, W. J., Shey, J., Imam, S. H., Glenn, G. M., Guttman, M. E., & Revol, J. F. (2005). Application of cellulose microfibrils in polymer nanocomposites. *Journal of Polymers and the Environment*, *13*, 301–306.

Saechtling, H. (1987). *International plastics handbook*. Munich: Hanser Gardner Publications.

Toyosaki, H., Naritomi, T., Seto, A., Matsuoka, M., Tsuchida, T., & Yoshinaga, F. (1995). Screening of bacterial cellulose-producing Acetobacter strains suitable for agitated culture. *Bioscience, Biotechnology and Biochemistry*, *59*, 1498.

Ummartyotin, S., Juntaro, J., Sain, M., & Manuspiya, H. (2012). Development of transparent bacterial cellulose nanocomposite film as substrate for flexible organic light emitting diode (OLED) display. *Industrial Crops and Product*, *1*, 92–97.

Valadez-Gonzalez, A., Cervantes-Uc, J. M., Olayo, R., & Herrera-Franco, P. J. (1999). Chemical modification of henequen fibers with an organosilane coupling agent. *Composites: Part B*, *30*, 321–331.

Yano, H., Sugiyama, J., Nakagaito, A. N., Nogi, M., Matsuura, T., Hikita, M., et al. (2005). Optically transparent composites reinforced with networks of bacterial nanofibers. *Advanced Materials*, *17*, 153–155.

Yoshinaga, F., Tonouchi, N., & Watanabe., K. (1997). Research progress in production of bacteria cellulose by aeration and agitation culture and its application as a new industrial material. *Bioscience, Biotechnology and Biochemistry*, *61*, 219–224.